Published OnlineFirst October 16, 2018; DOI: 10.1158/1078-0432.CCR-18-1278



Clinical Cancer Research

# Transcriptomic and Protein Analysis of Small-cell Bladder Cancer (SCBC) Identifies Prognostic Biomarkers and DLL3 as a Relevant Therapeutic Target

Vadim S. Koshkin[1,2], Jorge A. Garcia[1], Jordan Reynolds[3], Paul Elson[4], Cristina Magi-Galluzzi[3], Jesse K. McKenney[3], Kumiko Isse[5], Evan Bishop[5], Laura R. Saunders[5], Aysegul Balyimez[6], Summya Rashid[6], Ming Hu[4], Andrew J. Stephenson[7], Amr F. Fergany[7], Byron H. Lee[7], Georges-Pascal Haber[7], Afshin Dowlati[8], Timothy Gilligan[1], Moshe C. Ornstein[1], Brian I. Rini[1], Mohamed E. Abazeed[6,9], Omar Y. Mian[6,9], and Petros Grivas[1,10]

## Abstract

**Purpose:** Transcriptomic profiling can shed light on the biology of small-cell bladder cancer (SCBC), nominating biomarkers, and novel therapeutic targets.

**Experimental Design:** Sixty-three patients with SCBC had small-cell histology confirmed and quantified by a genitourinary pathologist. Gene expression profiling was performed for 39 primary tumor samples, 1 metastatic sample, and 6 adjacent normal urothelium samples (46 total) from the same cohort. Protein levels of differentially expressed therapeutic targets, DLL3 and PDL1, and also CD56 and ASCL1, were confirmed by IHC. A SCBC PDX model was utilized to assess *in vivo* efficacy of DLL3-targeting antibody–drug conjugate (ADC).

**Results:** Unsupervised hierarchical clustering of 46 samples produced 4 clusters that correlated with clinical phenotypes. Patients whose tumors had the most "normal-like" pattern of gene expression had longer overall survival (OS) compared with the other 3 clusters while patients with the most "metastasis-like" pattern had the shortest OS ($P = 0.047$). Expression of DLL3, PDL1, ASCL1, and CD56 was confirmed by IHC in 68%, 30%, 52%, and 81% of tissue samples, respectively. In a multivariate analysis, DLL3 protein expression on >10% and CD56 expression on >30% of tumor cells were both prognostic of shorter OS ($P = 0.03$ each). A DLL3-targeting ADC showed durable antitumor efficacy in a SCBC PDX model.

**Conclusions:** Gene expression patterns in SCBC are associated with distinct clinical phenotypes ranging from more indolent to aggressive disease. Overexpression of *DLL3* mRNA and protein is common in SCBC and correlates with shorter OS. A DLL3-targeted ADC demonstrated *in vivo* efficacy superior to chemotherapy in a PDX model of SCBC.
*Clin Cancer Res; 1–12. ©2018 AACR.*

## Introduction

Small-cell bladder cancer (SCBC) accounts for approximately 2% to 5% of all bladder tumors (1) and recent data suggest the "neuronal" subtype may be more common (2, 3). SCBC is associated with aggressive disease characterized by early progression and metastases. SCBC biology is poorly understood, but its clinical behavior shares similarities with small-cell and neuroendocrine tumors of other primary sites, such as small-cell lung cancer (SCLC; refs. 4, 5). It is estimated that 38% to 70% of SCBC exhibit coexisting non–small cell carcinoma, most commonly invasive and/or *in situ* urothelial carcinoma (6, 7). No standard of care based on randomized clinical trials exists for advanced SCBC, and treatments have been extrapolated from SCLC and bladder urothelial carcinoma (8–11). Several retrospective series (7, 12–15, 17) and small prospective trials (11, 16) have assessed treatment patterns and efficacy in SCBC. In general, early relapses are common with poor overall outcomes (1, 7, 18, 19). More effective therapies and more refined prognostic biomarkers are needed in SCBC.

[1]Department of Hematology and Medical Oncology, Cleveland Clinic, Cleveland, Ohio. [2]Division of Hematology and Oncology, Department of Medicine, University of California San Francisco, San Francisco, California. [3]Department of Anatomic Pathology, Cleveland Clinic, Cleveland, Ohio. [4]Department of Quantitative Health Sciences, Cleveland Clinic, Cleveland, Ohio. [5]Abbvie Stemcentrx, South San Francisco, California. [6]Department of Translational Hematology & Oncology Research, Cleveland Clinic, Cleveland, Ohio. [7]Department of Urology, Cleveland Clinic, Cleveland, Ohio. [8]Department of Hematology and Oncology, University Hospitals Cleveland Medical Center, Cleveland, Ohio. [9]Cleveland Clinic, Department of Radiation Oncology, Cleveland, Ohio. [10]University of Washington, Department of Medicine, Division of Oncology, Seattle, Washington.

**Note:** Supplementary data for this article are available at Clinical Cancer Research Online (http://clincancerres.aacrjournals.org/).

**Corresponding Authors:** Omar Y. Mian, Cleveland Clinic, 9500 Euclid Ave., Cleveland, OH 44195. Phone: 216-445-3273; Fax: 216-445-1068; E-mail: miano@ccf.org; and Petros Grivas, University of Washington/SCCA, 825 Eastlake Ave E, MS: G4830, Seattle, WA 98109. Phone: 206-606-7595; E-mail: pgrivas@uw.edu

**doi:** 10.1158/1078-0432.CCR-18-1278

Published OnlineFirst October 16, 2018; DOI: 10.1158/1078-0432.CCR-18-1278



## Translational Relevance

The biology of SCBC is not well defined and effective treatment options are limited. In this study, gene expression clustering separated SCBC tumors into groups associated with more aggressive or more indolent disease. We identified increased gene expression of *DLL3* (Delta Like Canonical Notch Ligand 3) in SCBC, and verified increased DLL3 protein expression by IHC in the tumor samples. Increased protein expression of DLL3 was associated with shorter overall survival in SCBC. DLL3 was separately assessed as a potential therapeutic target with preclinical data demonstrating efficacy of a DLL3-targeting antibody–drug conjugate (ADC) in a SCBC PDX model. Data support the potential utility of transcriptomic analysis in identifying clinically distinct molecular taxonomies in SCBC and nominate DLL3 as a potential therapeutic target. The ability to separate patients with SCBC into distinct prognostic groups may inform treatment and clinical trial design in SCBC.

SCBC is underrepresented in the TCGA, leading to separate studies exploring its unique genomic landscape (20, 21). New tumor biomarkers and therapeutic targets are emerging through extrapolation from other neuroendocrine malignancies. One example is delta-like protein 3 (DLL3), a Notch pathway ligand overexpressed on the surface of SCLC cells and other neuroendocrine malignancies (22, 23). This finding led to the development of a DLL3-targeted antibody–drug conjugate (ADC; ref. 24), Rovalpituzumab tesirine (Rova-T), consisting of a DLL3-targeted mAb conjugated to a DNA-damaging pyrrolobenzodiazepine (PBD) dimer toxin (Abbvie Stemcentrx, Inc.) with demonstrated efficacy in preclinical (23) and in an early-phase clinical trials (25). Programmed death ligand 1 (PDL1), expressed on immune and/or tumor cells is targeted by checkpoint inhibitors, FDA approved in urothelial carcinoma.

Previously reported data in SCLC involving both gene expression profiling (26–28) and clinical evaluation of a DLL3-targeting agent led us to consider analogous approaches in SCBC. We hypothesized that gene and protein expression analysis of SCBC samples would validate potential prognostic biomarkers and treatment targets, for example, DLL3, in SCBC. Our primary objective was to identify histologic biomarkers and novel gene expression classifiers to inform patient selection and clinical trial designs in SCBC. We further sought supporting evidence for the efficacy of novel agents active against targets of interest in preclinical models of SCBC.

## Methods

### Patient selection and clinicopathologic review

A total of 63 patients with SCBC and available clinical data, seen at Cleveland Clinic from 1993 to 2016, were identified on the basis of pathology records. Clinical and pathologic characteristics, treatment patterns, and response and outcome data were collected for all 63 patients. All tissues were independently reviewed for this analysis by an experienced genitourinary pathologist who confirmed the diagnosis of SCBC and quantitated the small-cell component of each tumor (SC%). The study was approved by the Cleveland Clinic Institutional Review Board and was conducted in accordance with guidelines laid out in the Declaration of Helsinki. Written consent from subjects was not required (waiver of consent was granted because of the retrospective nature of the study).

### Gene expression analysis

Sufficient tissue for gene expression analysis was available for 39 patients utilizing the HTG EdgeSeq Oncology Biomarker Panel Assay (HTG Molecular Diagnostics) with probes for 2,560 genes validated for *in situ* expression profiling of FFPE-archived specimens (29, 30). Other methodologies (RNAseq, microarrays) were excluded because of low-input amounts and a requirement for high-quality RNA extraction. Gene expression analysis was performed on a total of 46 tissue samples: 39 primary SCBC tumor samples, 1 metastatic sample, and 6 normal bladder tissue samples (from the same 39 patient cohort). The EdgeSeq assay is a targeted NGS approach that produces dispersed probe read counts amenable to RNAseq analysis pipelines (31). Analysis was performed via the RNAseq workflow (Partek Genomics Suite). R (version 3.2.3) was used for statistical analysis of expression data. FDR correction (FDR <5%) and adjusted $P$ values ($P < 0.05$) were used for selection of top differentially expressed genes; candidates were subsequently validated by IHC. All 39 patients included in the gene expression analysis had tissue samples available for IHC analyses. Hierarchical clustering was performed to determine Euclidian distance between 46 tissue samples based on the expression of 2,560 genes in the EdgeSeq OBP Assay. Kaplan–Meier and log-rank proportional hazards testing were used for survival analysis. One-way ANOVA was used to detect differentially expressed genes among tumor sample clusters. Paired $t$ test was used to detect differentially expressed genes between tumor and adjacent normal samples for the 6 patients with matched samples.

### IHC analyses

Of 63 patients, 53 had tumor tissue samples assessed for DLL3 protein expression via validated Ventana IHC Assay (Ventana Medical Systems) with anti-DLL3 antibody (SC16.65, Abbvie Stemcentrx; ref. 25). DLL3 expression was defined as percentage of tumor cells in a tissue sample that stained positive for DLL3. PDL1 staining was assessed in the 53-patient cohort using both SP263 and SP142 anti-PDL1 antibodies (Ventana Medical Systems). Positive PDL1 expression was defined as $\geq$1% of tumor-infiltrating cells (IC) staining positive for PDL1 using either antibody, based on the manufacturer's specifications (32, 33). The pathologist who interpreted PDL1 staining had received training on both PDL1 assays. Finally, within the 53-patient subset, 52 patients with adequate tissue had IHC staining for neuroendocrine markers ASCL1 and CD56 using Abbvie Stemcentrx SC72.201 and DAKO (123C3) antibodies, respectively. Simultaneous costaining of biomarkers was not technically feasible. Spearman correlations for associations among biomarkers as well as between biomarkers and relevant patient characteristics, including outcomes, were assessed.

### Outcomes analyses

Univariate and multivariate analyses were used to identify relevant pathologic characteristics and histologic biomarkers among the predictors of overall survival (OS) measured from diagnosis to time of death, progression-free survival (PFS)

Published OnlineFirst October 16, 2018; DOI: 10.1158/1078-0432.CCR-18-1278



measured from diagnosis to the first recurrence/progression or death, and time to progression (TTP) measured from diagnosis to recurrence/progression with death in the absence of recurrence/progression considered a competing risk. OS, PFS, and TTP were also separately calculated for patients who underwent cystectomy; in those, endpoints were measured from the time of cystectomy. Cox proportional hazards models (for OS and PFS) and Fine and Gray model (for TTP) were used in the univariate and multivariate analyses of clinical outcomes. A recursive portioning algorithm was used to identify cut-off points for biomarker expression (DLL3, PDL1, ASCL1, CD56, and SC%) that were associated with differences in outcomes for patients above and below these thresholds.

### Patient-derived xenograft testing

The *in vivo* efficacy of a DLL3-targeting agent was additionally assessed in a PDX model. BL100 PDX was developed from a cystectomy specimen of a high-grade neuroendocrine bladder carcinoma of a 67-year-old Caucasian female after informed consent. BL100 was propagated in 5- to 7-week-old female NOD/SCID mice (Charles River Laboratories) by subcutaneous implantation of dissociated cells into a single site near the lower mammary fat pad. Animal health was monitored daily, and mouse weights and tumor volumes were measured weekly. All animal studies were approved by the Stemcentrx Institutional Animal Care and Use Committee (IACUC; protocols SCAR-3-2008 and SCAR-5-2009) and performed in accordance with American Association for Laboratory Animal Science and AVMA Guidelines. Eight mice were randomized per treatment group so that each treatment group had average tumor volumes of 140 to 200 $mm^3$. Tumors were measured with digital calipers using 2 dimensions, long and short axis (mm), and tumor volume ($mm^3$) was calculated as the volume of a prolate ellipsoid: 0.5 × long axis × short $axis^2$. Each group was treated intraperitoneally with either vehicle control, a single dose of cisplatin (5 mg/kg) and etoposide (8 mg/kg) for days 1 to 3, a single dose of SC16LD6.5 (Rova-T) at 1.6 mg/kg or a single dose of isotype control ADC (HuIgG1LD6.5) at 1.6 mg/kg. The Rova-T dose used (1.6 mg/kg) was selected from 3 doses of Rova-T that were tested on the PDX model (0.4, 0.8, and 1.6 mg/kg). The data for 1.6 mg/kg dose were included because tumors from that cohort were used in the limiting dilution assay to determine impact on tumor-initiating cell frequency (described below). The 2 lower doses were additionally not found to be efficacious. Tumor volumes were assessed weekly.

### *In vivo* limiting dilution assays

To assess whether treatment targets tumor-initiating cells (TICs), further experiments were performed. Tumors were removed after euthanasia 7 days posttreatment of 2 representative mice from each treatment group. Cohorts of 10 mice per group were injected with decreasing numbers of isolated BL100 tumor cells previously treated with either vehicle, isotype control, or Rova-T and ranging from 3,000 to 100 cells per recipient animal. Mice were scored positive for tumor growth if tumors exceeded 200 $mm^3$. This serial transplantation of cells from treated mice allowed for the estimation of residual TIC frequency using

**Table 1.** Baseline patient characteristics in the overall cohort and among patients with gene expression data (left) and pathologic characteristics among patients with cystectomies (right)

| Variable | All Patients ($N = 63$) | Patients with data on gene expression ($N = 39$) | Pathologic features of cystectomy patients | All cystectomy patients ($N = 41$) | Cystectomy patients with data on gene expression ($N = 27$) |
|---|---|---|---|---|---|
| Median age | 71 (39–90) | 70 (46–89) | Tumor location | | |
| | | | Bladder | 37 (90%) | 25 (92%) |
| | | | Bladder and ureter | 2 (5%) | 1 (4%) |
| | | | Bladder and urethra | 1 (2%) | 0 |
| | | | No tumor (T0) | 1 (2%) | 1 (4%) |
| ECOG PS at diagnosis | | | | | |
| 0 | 22 (35%) | 11 (28%) | Pathologic T-stage | | |
| 1 | 10 (16%) | 8 (21%) | T0–T2 | 15 (37%) | 9 (33%) |
| 2 | 4 (6%) | 3 (8%) | T3–T4 | 26 (63%) | 18 (67%) |
| 3 | 3 (5%) | 3 (8%) | | | |
| Unknown | 24 (38%) | 14 (36%) | | | |
| Gender | | | Pathologic N-stage | | |
| Male | 52 (83%) | 33 (85%) | N0: | 23 (56%) | 17 (63%) |
| Female | 11 (17%) | 6 (15%) | N1–N3: | 18 (44%) | 10 (37%) |
| Current/former smoker | | | Surgical margins | | |
| Yes | 44 (70%) | 29 (74%) | Positive | 8 (20%) | 6 (22%) |
| No | 15 (24%) | 6 (16%) | Negative | 29 (70%) | 18 (67%) |
| Unknown | 4 (6%) | 4 (10%) | Unknown | 4 (10%) | 3 (11%) |
| Hydronephrosis | | | Carcinoma *in situ* (CIS) | | |
| Yes | 9 (14%) | 7 (18%) | Present | 24 (59%) | 14 (52%) |
| No | 53 (84%) | 32 (82%) | Absent | 16 (39%) | 12 (44%) |
| Unknown | 1 (2%) | 0 | Unknown | 1 (2%) | 1 (4%) |
| | | | Lymphovascular invasion (LVI) | | |
| | | | Yes | 17 (41%) | 13 (48%) |
| | | | No | 10 (24%) | 5 (19%) |
| | | | Unknown | 14 (35%) | 9 (33%) |

NOTE: Left, patient characteristics at the time of initial SCBC diagnosis in the overall 63 patient cohort and among 39 patients who had gene expression data available; right, pathologic characteristics of cystectomy samples among patients who had a cystectomy at some point in their treatment course.

Published OnlineFirst October 16, 2018; DOI: 10.1158/1078-0432.CCR-18-1278



Poisson distribution statistics. Estimates of TIC frequency were calculated using the L-Calc software package (Stem Cell Technologies) to apply Poisson distribution analysis to the frequencies of tumor-negative mice at each injected cell number.

## Results

### Clinical, pathologic, and treatment characteristics

In the overall 63-patient cohort, median age was 71, 83% were men, 51% had ECOG Performance Status 0–1, 70% were current/former smokers; 41 patients underwent radical cystectomy and their pathologic characteristics are shown in Table 1. The subset of 39 patients whose tissue samples were available for gene expression analysis had similar baseline characteristics to the overall cohort (Table 1). Among all 63 patients, SCBC was diagnosed on TURBT for 48 and on cystectomy for 15. At initial diagnosis, 6 patients had distant metastases and 44% (18/41) of patients who had radical cystectomy with lymph node dissection had nodal metastasis. The full description of diagnosis and treatment patterns as well as most commonly used treatment regimens is available in Supplementary Materials (Supplementary Fig. S1; Supplementary Table S1).

### Gene expression profiling

Gene expression profiling was performed on 39 primary SCBC tumor samples with sufficient tissue. In 6 of those patients, gene

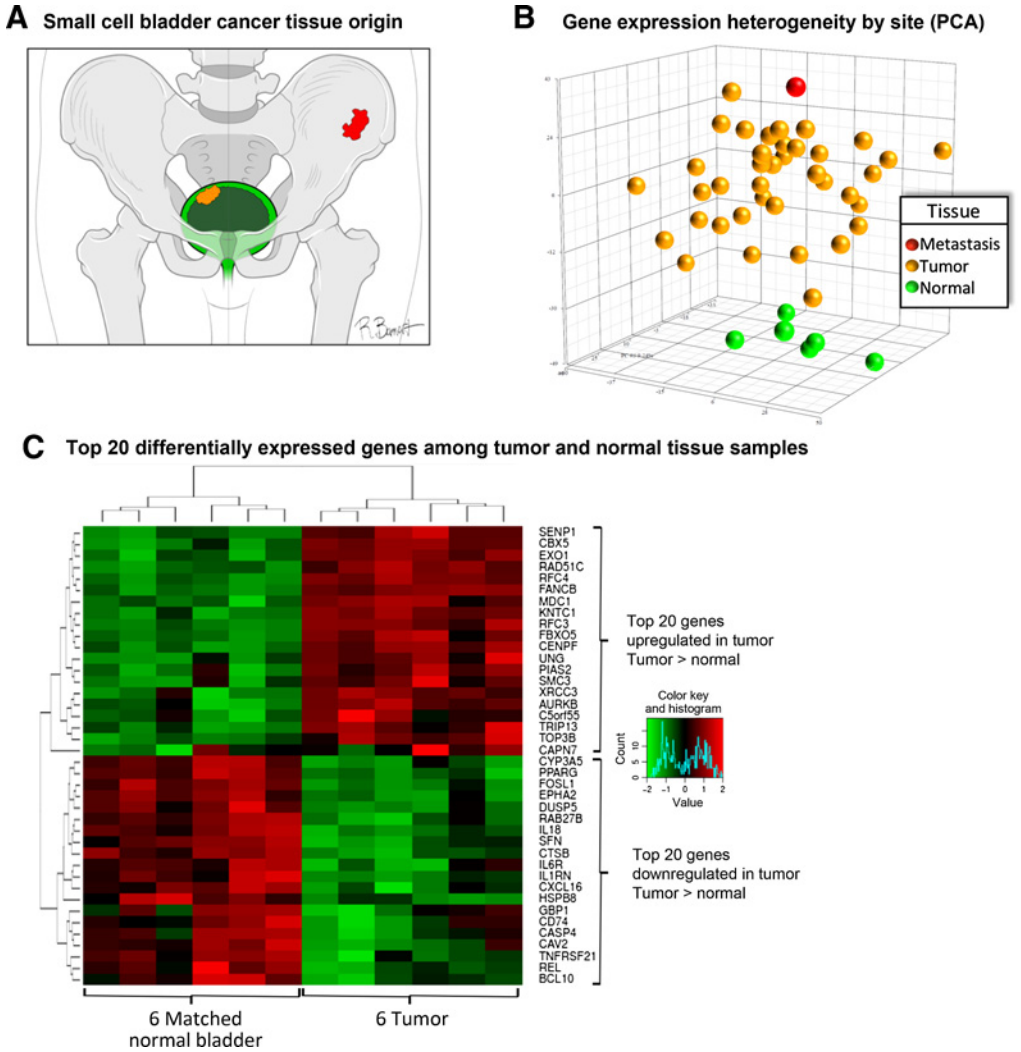


**Figure 1.**

**A,** Diagram of the tissues of origin utilized in the gene expression analysis. Green represents normal urothelial tissue samples, yellow represents tissue samples from primary bladder tumor, and red represents tissue from metastatic sample (osseous metastasis). **B,** Three-dimensional representation of the principal component analysis, which represents tissue gene expression heterogeneity across 2,560 genes as a Euclidian distance in 3 principal components. This displays a similarity in gene expression among normal urothelial samples (green), which stand apart from the gene expression similarity observed across primary small-cell bladder tumors (yellow), and finally apart from gene expression in the one metastatic sample (red), which is one of the gene expression outliers. **C,** Differential gene expression analysis comparing gene expression in 6 matched tumor and normal urothelial samples from the same patients. Top of the panel displays the top 20 genes with increased expression in tumor relative to normal samples, while the bottom panel displays the top 20 genes with greater expression in normal samples as compared with tumor samples.

Published OnlineFirst October 16, 2018; DOI: 10.1158/1078-0432.CCR-18-1278



expression profiling was also performed on matched adjacent "normal-appearing" urothelial tissue. Analysis of a single metastatic tissue was also performed (Fig. 1A). Principal components analysis of gene expression parameters for each of the 46 analyzed samples is depicted in Fig. 1B and displays grouping of expression profiles by tissue origin (tumor, normal, and metastatic).

Unsupervised hierarchical clustering of gene expression patterns from all 46 samples produced 4 distinct gene expression clusters (Fig. 2A). Consensus (K-means) clustering confirmed 4 distinct subsets (Supplementary Fig. S2). Importantly, membership within clusters was associated with discrete clinical phenotypes that correlated with OS (Fig. 2C). Patients with tumor

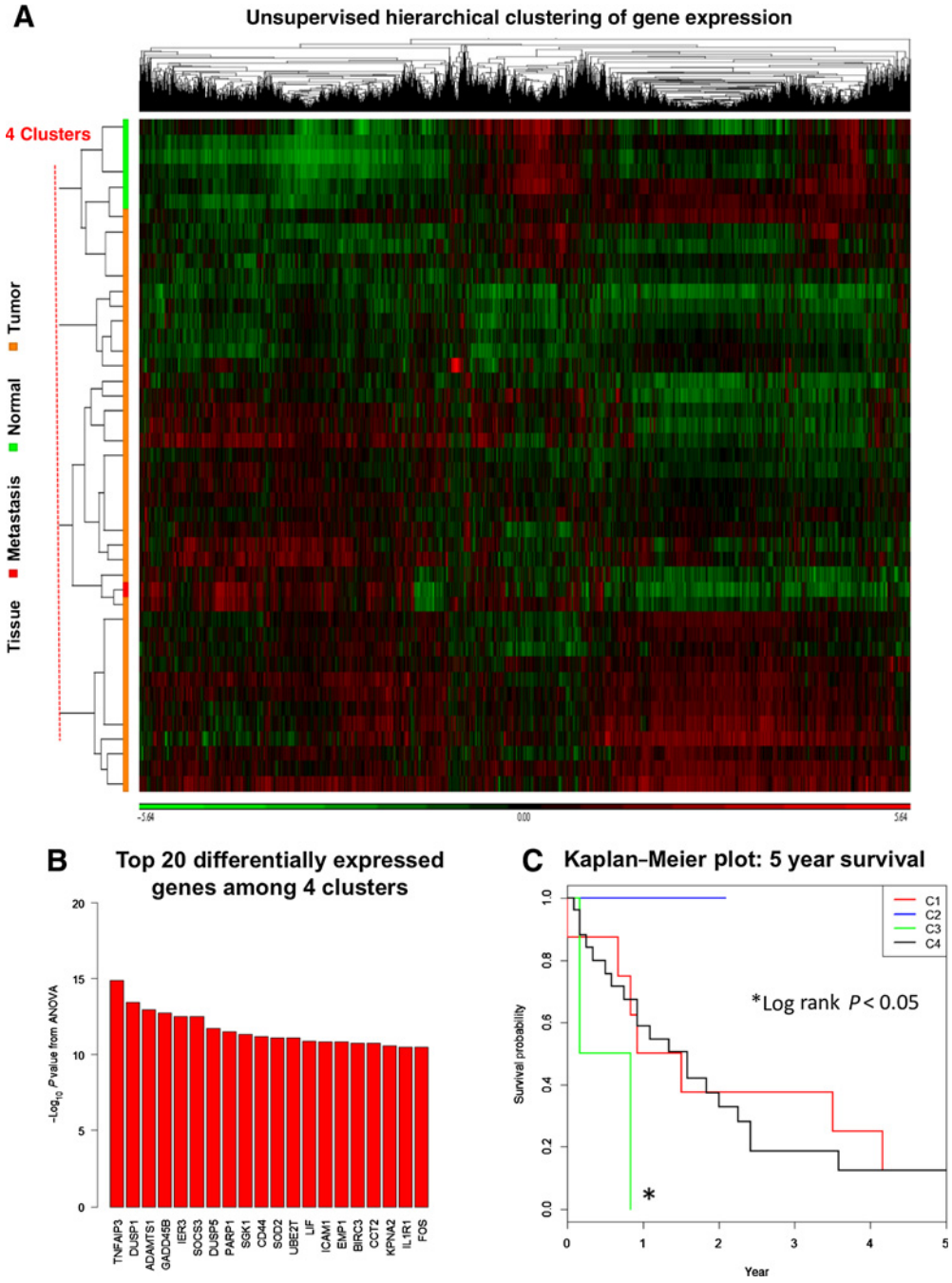


**Figure 2.**

**A,** Unsupervised hierarchical clustering separates individual tissue samples (rows on vertical axis), based on relative overexpression (green) or underexpression (red) of individual genes on the horizontal axis, into 4 distinct clusters of similar gene expression patterns. **B,** Top differentially expressed genes among 4 clusters. **C,** Kaplan–Meier plot of OS for patients across 4 identified gene expression clusters. Gene expression clusters correlate with distinct clinical phenotypes as patients with tumors in most "normal-like" C2 had superior OS, whereas patients in the most "metastasis-like" C3 have shorter OS (median OS 6.0 months) compared with the other 3 clusters (log rank $P = 0.047$).

Published OnlineFirst October 16, 2018; DOI: 10.1158/1078-0432.CCR-18-1278



samples in cluster 2, containing all 6 normal urothelial tissue samples, had the most favorable clinical phenotype. The coclustered tumor and normal samples originated from different patients, suggesting greater similarity between clinically indolent tumors and normal tissues than between tumor and normal tissues from a single individual. Patients in cluster 2 did not develop metastasis. On the other hand, patients in cluster 3 whose tumors had a gene expression pattern that grouped them with the metastatic tumor sample, were more likely to have metastasis and had shorter median OS (6 months) compared with patients in the other 3 clusters (Kaplan–Meier log-rank $P = 0.047$). The top 20 differentially expressed genes among the 4 clusters (associated with the highest ANOVA *P* values) are shown in Fig. 2B. Gene set enrichment analysis (GSEA) for top 200 differentially expressed genes among the 4 clusters demonstrated distinct dominant biological networks (Supplementary Fig. S3).

Among the 6 matched pairs of tumor and adjacent normal tissue from the same patient, the differential gene expression analysis using matched pairs resulted in a total of 583 differentially expressed genes with FDR <0.05. The top differentially expressed genes (based on *P* value) for the tumor versus normal tissue comparison and the associated heatmap are shown in Fig. 1C, while the GSEA plots are available in Supplementary Fig. S4. *EZH2*, which is overexpressed or mutated in numerous malignancies and targeted by an agent being tested in clinical trials (34) was significantly overexpressed in the 6 SCBC tumors compared with normal tissue samples ($P = 0.0003$; Fig. 3D). This finding is consistent with prior reports of *EZH2* and associated polycomb repressor group (PRC) dysregulation in SCLC (35, 36).

Among genes with significantly higher mRNA expression in SCBC tumor samples relative to normal urothelial tissue, *DLL3* ($P = 0.02$) and *NCAM1*(CD56; $P = 0.007$) represented potential biomarkers of interest given their prior association with other small cell- or neuroendocrine malignancies, and in the case of DLL3, the availability of Rova-T (Fig. 3A–C). Expression of DLL3, CD56, and other proteins was then assessed in patients with available tumor samples (see below). Among all 2,560 genes in the HTG EdgeSeq panel, DLL3 protein expression was most strongly correlated with expression of *DLL3* mRNA (Supplementary Fig. S5), suggesting that regulation of *DLL3* expression occurs primarily at the transcriptional rather than the translational level.

### Biomarker expression and small-cell component

Gene expression analysis identified candidate proteins for further investigation as relevant biomarkers of interest. All 63 SCBC tumors had confirmed small-cell component (SC%) with a range of 5% to 100%; 59% of tumors had SC% of 100% (pure small cell histology) and 79% had SC% of ≥50% (small cell as dominant histology). Among patients with a mixed histology, urothelial carcinoma was the most common non–small cell histology. Among 39 patients with available gene expression data, SC% had a significant correlation with mRNA expression of *DLL3* ($r = 0.68$; $P = 0.02$) and *CD56* ($r = 0.42$; $P = 0.008$).

In 53 patients with available tissue specimens for IHC of DLL3 (therapeutic target of Rova-T) and PDL1 (therapeutic target of checkpoint inhibitors), DLL3 protein expression (≥1% of tumor cells) on IHC was noted in 68% of patients, with 58% having expression in >10% of tumor cells (Fig. 4). The median percentage of DLL3-positive tumor cells among all samples was 40% (range 0%–100%). There was a positive correlation between percentage of DLL3-positive tumor cells and SC% of tumor (Spearman $r = 0.33$; $P = 0.01$), *DLL3* mRNA expression ($r = 0.70$; $P = 1.0 \times 10^{-7}$), and mRNA expression of neuroendocrine markers and Notch pathway proteins including *DLL4* ($r = 0.44$; $P = 0.004$) and *CHGA* ($r = 0.55$; $P = 0.0003$). A negative correlation was noted between DLL3 IHC and mRNA expression of *Notch1* ($r = -0.47$; $P = 0.002$), *RB1* ($r = -0.48$; $P = 0.002$), and *EZH2* ($r = -0.29$; $P = 0.07$). PDL1 protein expression via IHC was only noted on tumor-infiltrating immune cells and not on tumor cells. In 30% of available samples, PDL1 expression was seen on ≥1% of tumor-ICs using either SP263 or SP142 anti-PDL1 antibodies (21% for SP263 alone, 2% for SP142 alone, and 7% for both SP263 and SP142). However, no case reached previously defined criteria for either high or positive expression for SP263 or SP142 antibody, respectively, due to lack of tumor cell or IC staining in the remaining tumor microenvironment. No significant correlation was noted between PDL1 protein expression and either DLL3 protein expression, SC%, or outcomes.

Among 53 patients with IHC of DLL3 and PDL1, 52 patients also had tissue samples available for IHC of CD56/NCAM1 and ASCL1(1 patient excluded due to artifact). Positive cell membrane expression of CD56/NCAM1 protein (≥1% of tumor cells) was observed in 81% of tumors (Fig. 4). The median percentage of CD56-positive cells in tumor tissue was 65% (range 0–100%), and lower CD56 expression was noted in patients older than age 70 ($P = 0.05$). CD56/NCAM1 protein expression was correlated with SC% ($r = 0.26$; $P = 0.06$), DLL3 protein expression ($r = 0.32$; $P = 0.02$), and with mRNA expression of neuroendocrine markers including *NCAM1* ($r = 0.61$; $P = 0.00003$), *DLL4* ($r = 0.38$; $P = 0.017$), *Notch1* ($r = -0.34$; $P = 0.034$), and *SYP* ($r = 0.34$; $P = 0.033$). Positive expression of ASCL1 transcription factor (≥1% of tumor cells) was observed in 52% of tumor tissues but the median percentage of ASCL1-positive cells within a tumor was only 10% (range 0%–100%). ASCL1 protein expression had strong correlation with protein expression of DLL3 ($r = 0.73$; $P = 0.00001$) and moderate correlation with expression of CD56 ($r = 0.35$; $P = 0.01$) and SC% ($r = 0.34$; $P = 0.01$). Significant correlation of ASCL1 protein expression with mRNA expression of several Notch pathway proteins and neuroendocrine markers was observed including *DLL3* ($r = 0.46$; $P = 0.0035$), *DLL4* ($r = 0.60$; $P = 0.00005$), *CHGA* ($r = 0.41$; $P = 0.01$), *Notch1* ($r = -0.34$; $P = 0.002$), and *EZH2* ($r = -0.31$; $P = 0.05$).

### Clinical outcomes and prognostic factors

In the overall 63-patient cohort, the median follow-up was 16.6 months from the time of tissue-confirmed diagnosis of SCBC. Median OS was 22.8 months (95% CI, 11.9–42.4) and median PFS was 13.7 months (95% CI, 11.2–19.4). Multivariate analyses revealed several independent prognostic factors for OS, PFS, and TTP in this cohort (Fig. 4). Increased DLL3 protein expression, with a determined cutoff of >10% of cells based on a recursive portioning algorithm, was associated with shorter OS and PFS from diagnosis and shorter OS from cystectomy ($P \leq 0.05$ for all). Increased CD56/NCAM1 protein expression (>30% of tumor cells) was similarly associated with shorter PFS (HR: 2.07; 95% CI, 1.02–4.20; $P = 0.04$) and OS (HR: 2.23; 95% CI, 1.06–4.70; $P = 0.03$). A subset of 9 patients whose tumor samples had low

Published OnlineFirst October 16, 2018; DOI: 10.1158/1078-0432.CCR-18-1278



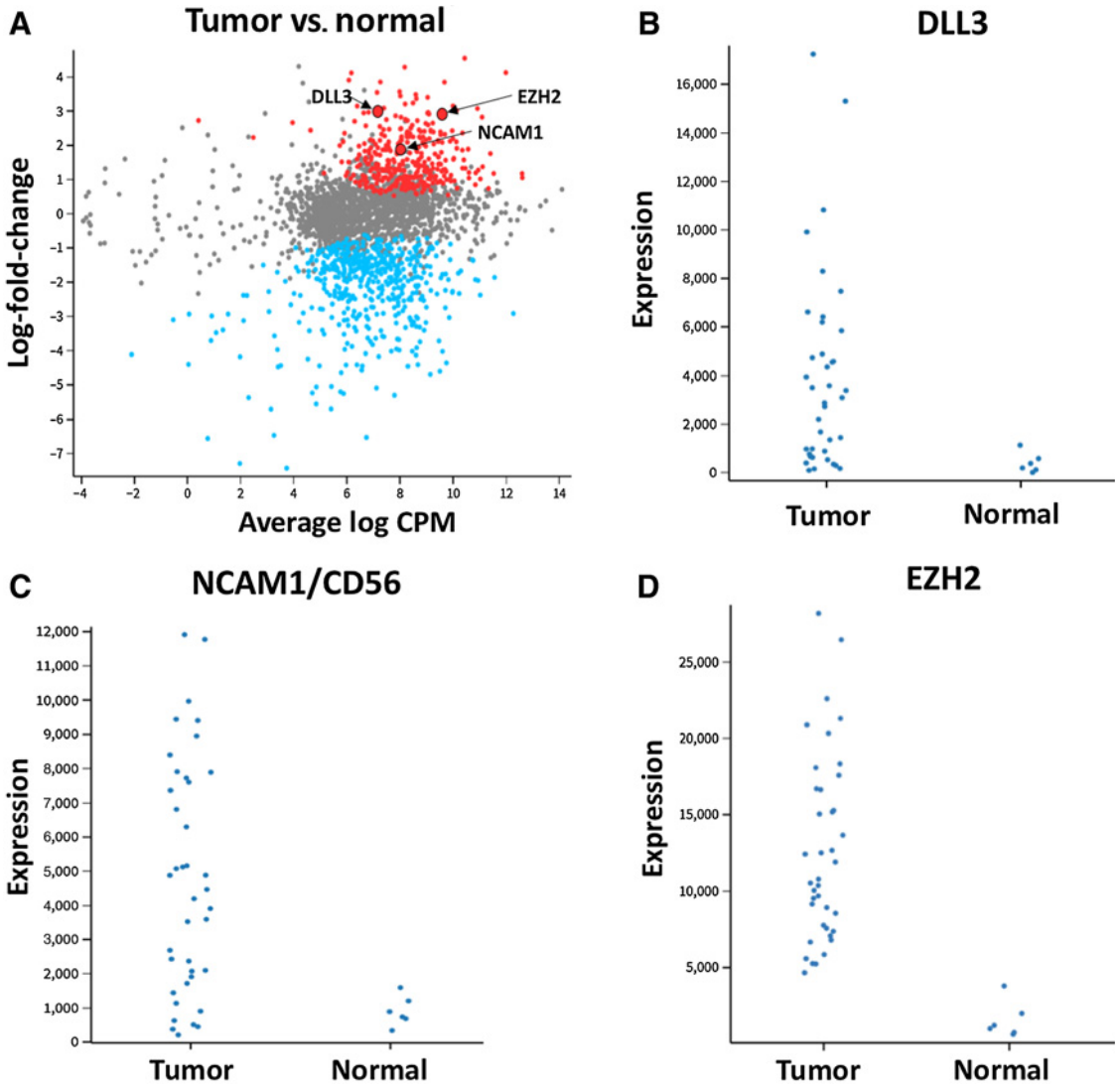


**Figure 3.**

**A,** Gene expression log fold change versus average log of counts per million (CPM) across samples; significantly differentially expressed genes (log fold change >1.0, $P_{adj} < 0.05$) are displayed in red if upregulated and blue if downregulated in tumors versus normal. Arrows highlight genes of interest. Plots for DLL3 (**B**), NCAM1/CD56 (**C**), and EZH2 (**D**) display gene expression in individual tumor and available normal samples.

expression of both DLL3 (≤10%) and CD56 (≤30%) had significantly longer OS (103.4 vs. 18.4 months; $P = 0.01$) and PFS (92.2 vs. 11.4 months; $P = 0.02$) relative to patients with high protein expression of either biomarker. On the other hand, increased SC component (>50%) was not associated with OS, but was associated with shorter PFS from cystectomy ($P = 0.02$) and shorter TTP from cystectomy ($P = 0.03$). Neither PDL1 nor ASCL1 protein expression assessed via IHC had association with survival outcomes in this cohort. Pathologic T3/4 stage at cystectomy was associated with shorter OS from the time of cystectomy compared with pT1/T2 ($P = 0.05$). Positive margin status at cystectomy had a trend toward shorter PFS from cystectomy, although this finding did not reach statistical significance ($P = 0.06$). Kaplan–Meier plots of OS and PFS for significant prognostic factors are depicted in Fig. 4.

### Preclinical efficacy of DLL3-targeting agent

With DLL3 protein expression shown to be common in SCBC samples and potentially prognostic of poor outcomes, we pursued assessment of the preclinical efficacy in a PDX model of a novel agent (Rova-T) that exploits the expression of DLL3 on the surface of SCBC tumor cells to deliver a cytotoxic agent. FFPE samples of a SCBC PDX model, BL100, were stained by IHC with antibodies specific to DLL3 and shown to express DLL3 on the surface of all tumor cells (Fig. 5A). Rova-T was assessed for *in vivo* efficacy in these models. As described, following implantation of BL100 tumor cells into 4 groups of NOD/SCID mice, each group was treated with either vehicle control, a single dose of cisplatin plus etoposide on days 1 to 3, a single dose of SC16LD6.5 (Rova-T), or an isotype antibody control ADC (HuIgG1LD6.5; Fig. 5B). Neither vehicle nor cisplatin/etoposide impeded tumor growth,

Published OnlineFirst October 16, 2018; DOI: 10.1158/1078-0432.CCR-18-1278



while the isotype ADC showed nonspecific response that repressed tumor growth for only approximately 50 days. A single dose of Rova-T, on the other hand, prevented tumor growth for >100 days, providing durable and specific antitumor response (Fig. 5C). No significant treatment-related toxicities were observed in the mice.

To determine whether Rova-T prevents recurrence by targeting TICs, tumors were harvested from 2 mice in each treatment group and limiting dilutions of isolated BL100 cells were retransplanted into cohorts of 10 mice per treatment. Vehicle-treated BL100 PDX tumors had TIC frequency around 1:252 cells, which was reduced to approximately 1:365 by HuIgG1LD6.5 treatment, and

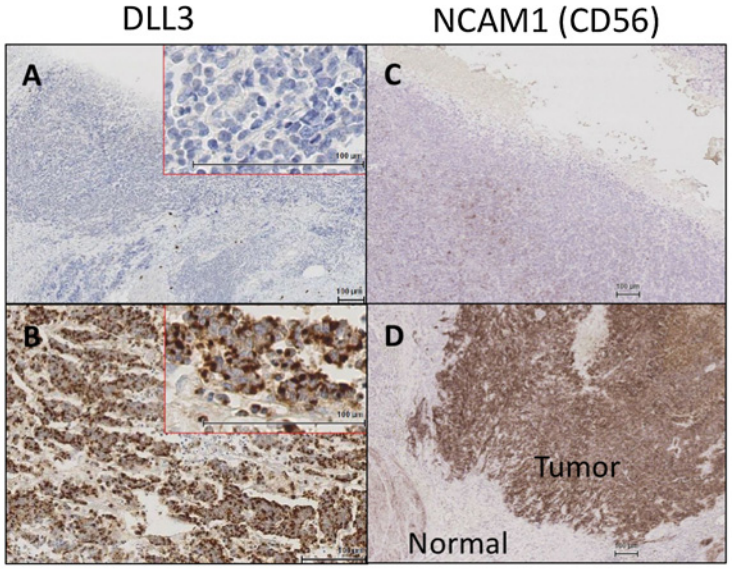


| Overall Survival (OS) | | |
|---|---|---|
| Factor | HR (95% CI) | *P* |
| % cells DLL3+ (>10% vs. ≤10%) | **2.8** (1.1–6.7) | 0.03 |
| % cells CD56+ (>30% vs. ≤30%) | **2.2** (1.1–4.7) | 0.03 |
| pT Stage (T3/T4 vs. T1/T2)* | **2.5** (1.0–6.2) | 0.05 |
| **Progression-free survival (PFS)** | | |
| Factor | HR (95% CI) | *P* |
| % cells (DLL3+) (>10% vs. ≤10%) | **2.5** (1.1–5.8) | 0.04 |
| % cells CD56+ (>30% vs. ≤30%) | **2.1** (1.02–4.2) | 0.04 |
| Small cell % (>50% vs. ≤50%)* | **3.6** (1.2–10.9) | 0.02 |
| Margins (positive vs. negative)* | **2.3** (1.0–5.3) | 0.06 |
| **Time to progression (TTP)** | | |
| Factor | HR (95% CI) | *P* |
| % Small cell (>50% vs. ≤50%)* | **4.0** (1.1–14.4) | 0.03 |

*pT Stage, small cell % and margin status outcomes measured from time of cystectomy

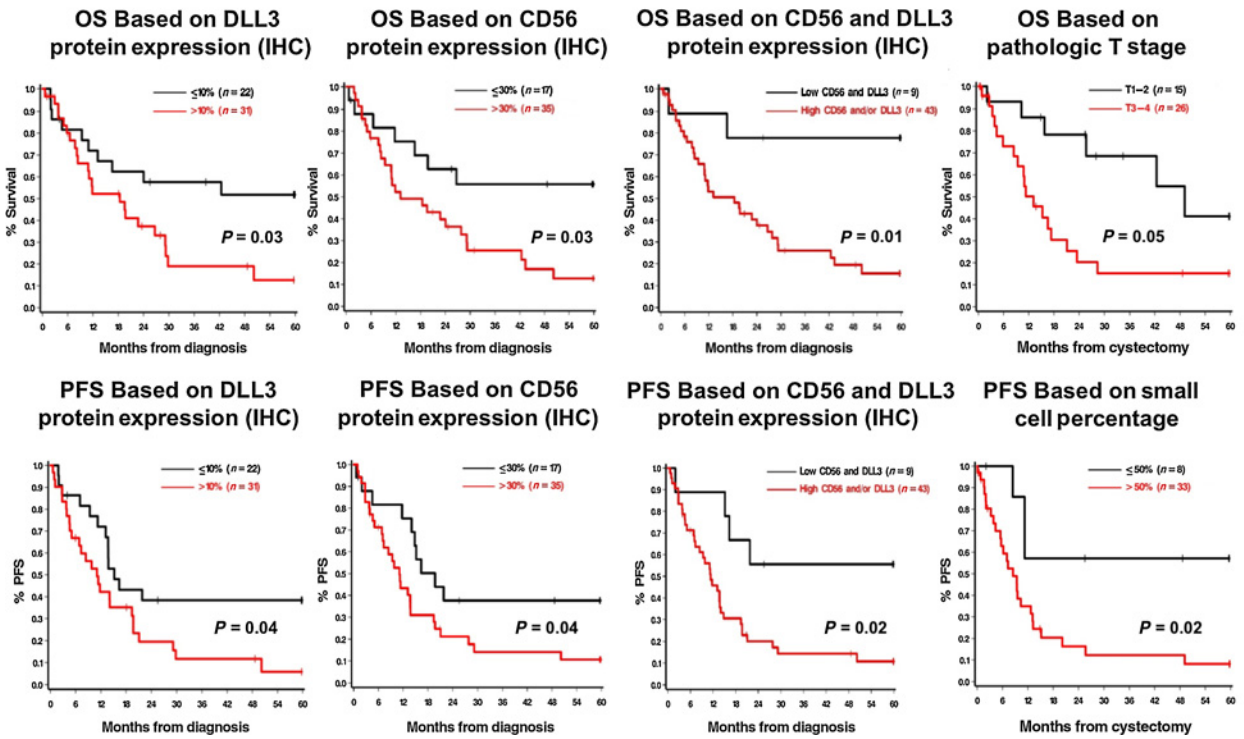


**Figure 4.**

Top left, IHC for DLL3 expression: negative control (**A**) and tissue with 95% of tumor cells expressing DLL3 (**B**). IHC for CD56 expression: negative control (**C**) and tissue (**D**) with 70% of tumor cells expressing CD56. Top right, multivariate analyses of tumor characteristics associated with relevant clinical outcomes including OS, PFS, and time to progression. Bottom, Kaplan–Meier plots and associated *P* values for OS and PFS based on predetermined cut-off points for tumor markers and other characteristics.

Published OnlineFirst October 16, 2018; DOI: 10.1158/1078-0432.CCR-18-1278



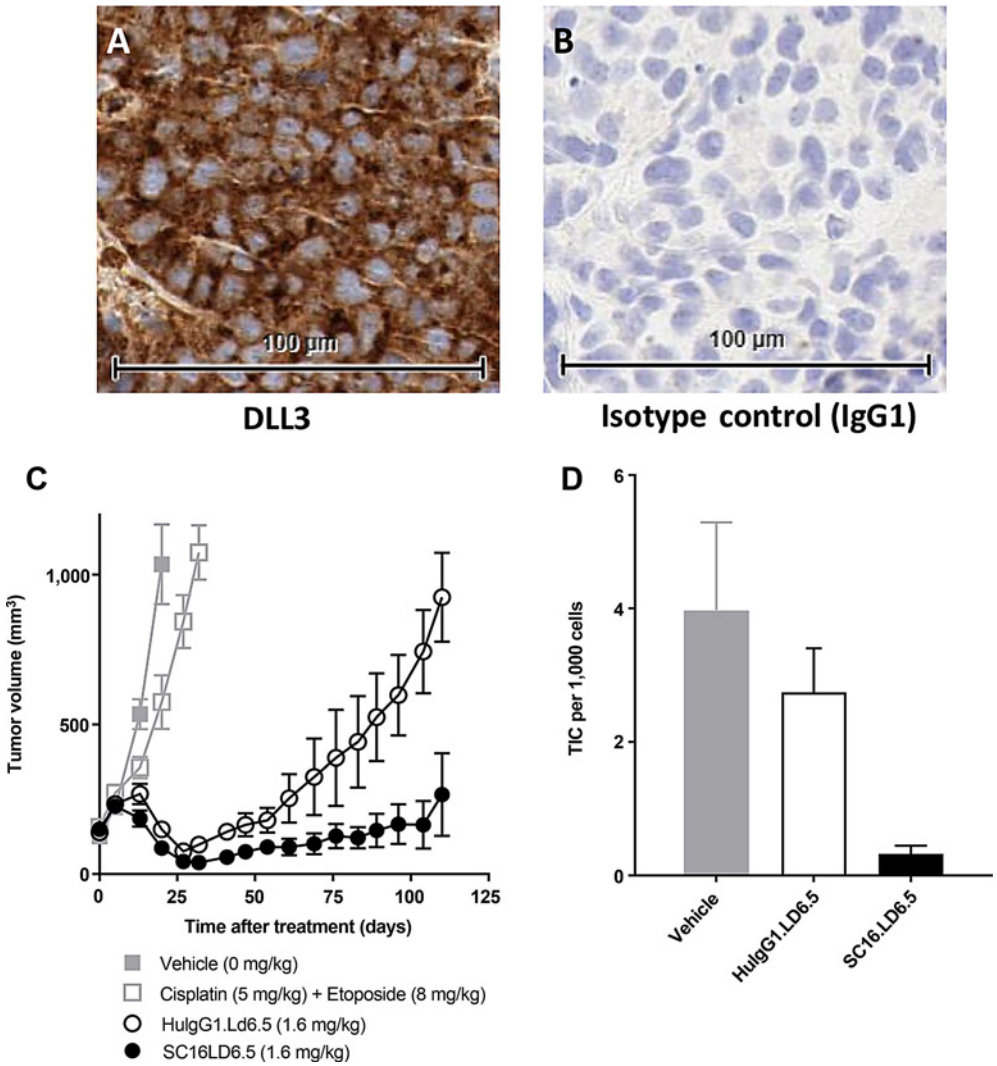


**Figure 5.**

DLL3 IHC of FFPE sample of a SCBC patient-derived xenograft (PDX) model (**A**) and isotype control (IgG1) of same FFPE sample showing lack of staining (**B**). **C,** Tumor volumes across time in 4 groups of NOD/SCID mice implanted with BL100 tumor cells (SCBC PDX model) and treated with either vehicle, cisplatin/etoposide, SC16LD6.5 (antibody–drug conjugate Rova-T), or hulgG1LD6.5 (isotype antibody control ADC). **D,** Estimated residual tumor-initiating cell (TIC) frequency in tumors previously treated with vehicle, HulgG1LD6.5 or SC16LD6.5, suggesting that TIC suppression by SC16LD6.5 (Rova-T) is the mechanism that induces durable responses to Rova-T treatment.

significantly reduced to approximately 1:3036 by a single dose of Rova-T (Fig. 5D). Collectively, these experiments support durable *in vivo* efficacy of Rova-T, which effectively targets DLL3-expressing TICs in a SCBC PDX model.

## Discussion

We report one of the largest studies of gene expression profiling in SCBC and the first to assess the prognostic value of differentially expressed proteins associated with neuroendocrine differentiation, including DLL3, ASCL1, CD56/NCAM1, and PDL1. We identified a gene expression cluster associated with aggressive biology in SCBC with a distinct molecular taxonomy associated with poor prognosis. In addition, DLL3 and CD56/NCAM1 were identified as negative prognostic biomarkers in SCBC, and DLL3 was further validated as a potential therapeutic target with preclinical evidence supporting *in vivo* efficacy of a DLL3-targeting ADC in a SCBC PDX model. These data have implications for future therapeutic strategies in SCBC.

All patients in this study had small-cell histology independently confirmed and quantitatively defined by an experienced genitourinary pathologist. Although SCBC was not included in the original TCGA analysis of bladder cancer published in 2014 (37), several recent studies including the updated TCGA analysis published in 2017 (2), have added to our understanding of the SCBC genomic landscape. These studies highlight similarities of SCBC to SCLC as well as important differences (20, 28, 38). Recently published data suggest that SCBC and SCLC have a convergent but distinct pathogenesis, with SCBC having high somatic mutational burden driven by APOBEC mutations, also commonly found in

Published OnlineFirst October 16, 2018; DOI: 10.1158/1078-0432.CCR-18-1278



urothelial carcinoma, which may precede *TP53* and *RB1* mutations that typify small-cell malignancies (38). The notable high incidence and role of APOBEC mutagenesis is currently unknown and merits further investigation with respect to its relationship with DLL3 expression in SCBC.

Available genomic datasets in bladder cancer have largely focused on the more common urothelial histology. The updated TCGA analysis of 412 muscle-invasive bladder cancers included only 4 tumors with neuroendocrine histology. Three of these 4 tumors clustered with the "neuronal" molecular subtype that included an additional 17 tumors (20 total) without histopathologic features of neuroendocrine origin. The "neuronal" molecular subtype was characterized by typical neuroendocrine markers as well as frequent loss or mutation of *TP53* and *RB1* and high expression of neuronal differentiation and development genes. Consistent with the known aggressive clinical phenotype of small-cell and neuroendocrine bladder cancers, the neuronal subtype had the poorest survival among the 5 molecular subtypes identified in the updated TCGA analysis (2). These findings support the notion that integrative molecular profiling of tumor samples may complement the histopathologic diagnosis of SCBC, as most neuronal subtype tumors lacked small-cell or neuroendocrine histology. Our results further substantiate this premise by demonstrating an association between gene expression signatures and clinical behavior among histologically confirmed SCBC samples. Acknowledging the relatively small number of patients and inherent limitations of retrospective analysis, these findings should be regarded as hypothesis-generating. Comparisons of gene expression data from our analysis with the TCGA dataset and data from additional SCBC cohorts are currently being pursued.

In our analysis, unsupervised hierarchical clustering of gene expression profiles for 39 tumor samples, 6 matched "normal" bladder tissue samples and 1 metastatic site sample revealed 4 stable gene expression clusters that correlated with clinical phenotypes. We included normal samples in the clustering analysis to assess their inherent similarity and determine the intraindividual transcriptomic differences between tumor and adjacent "normal-appearing" tissues. Recognizing the limitations of assessing the "normal" adjacent tissue in the context of field cancerization and tumor heterogeneity, a number of provocative patterns emerged from this gene expression analysis. For instance, the single metastatic sample clustered closely with the primary tumor sample from the same patient. In contrast, the 6 primary tumors and their 6 matched normal tissue samples did not reliably cluster together. One interpretation is that gene expression among SCBC samples from different individuals may converge on a common transcriptional program, appearing more closely related than expression patterns in matched tumor and normal tissue samples from the same patient. This observation supports prior findings in urothelial carcinoma, demonstrating shared early "truncal" events in the course of tumorigenesis and subsequent convergent clonal evolution (39). The similarity of gene expression patterns in the metastatic sample with the primary tumor from which it arose and with another primary tumor from a patient with similarly poor outcome further supports convergent evolution toward more aggressive disease phenotype. On the other hand, tumor samples that clustered closely with normal samples—or had a more "normal-like" pattern of gene expression demonstrated more indolent clinical course. Taken together, these data suggest that membership in specific gene expression clusters may reflect underlying biology explaining their prognostic value for individual patients. These findings, while provocative, remain to be validated prospectively and are limited in the present dataset by the availability of a single metastatic sample. Identifying the specific genetic determinants of a "metastasis-like" or "normal-like" expression signature in SCBC represents the next logical step in developing risk stratification models to guide management. The differential gene expression appears to be driven by overlapping gene networks, and functional studies are ongoing to better define pathways involved and their role in modulating clinical phenotypes.

We confirmed a strong correlation between mRNA and protein expression of DLL3 and similar findings with CD56/NCAM1. These findings confirmed our hypothesis that regulation of these proteins in SCBC likely occurs at the transcriptional rather than translational level. Our results indicate that the expression of ASCL1 and CD56/NCAM1 proteins in SCBC tumors is also correlated with mRNA expression of several Notch pathway proteins and proteins related to neuroendocrine differentiation such as *DLL3*, *DLL4*, *Notch 1*, *CHGA*, and *SYP*. Furthermore, efforts to better characterize these pathways and the underlying biological mechanisms in SCBC are ongoing.

The expression of DLL3, a promising treatment target in early-phase clinical trials in SCLC and other neuroendocrine malignancies, has not been previously reported in SCBC. The majority (68%) of SCBC tumors in our cohort had positive DLL3 protein expression, which is similar to SCLC and other solid malignancies, such as melanoma, glioblastoma, and medullary thyroid cancer (40). This is the first study to report increased DLL3 and CD56 expression as independent negative prognostic biomarkers in SCBC associated with shorter PFS and OS in multivariate analyses. Conversely, low simultaneous IHC expression of both DLL3 and CD56 may identify long-term SCBC survivors, as 9 patients that met these criteria had median OS exceeding 100 months.

In addition to being a prognostic biomarker in SCBC, DLL3 expression may be an important predictive biomarker and treatment target. A phase I trial of Rova-T, the ADC that exploits DLL3, in a heavily pretreated population of patients with SCLC and large-cell neuroendocrine carcinoma showed robust response in patients with limited treatment options (25). A clinical trial of Rova-T in DLL3-expressing solid tumors is ongoing (NCT02709889) and includes patients with SCBC in one of the neuroendocrine carcinoma cohorts (41). The high proportion of SCBC tissue samples expressing DLL3 in a high percentage of tumor cells suggests the potential clinical utility of DLL3-targeted agents in this population. Our preclinical data demonstrating Rova-T efficacy in DLL3-expressing SCBC PDX models are further supportive. Prior studies have shown Rova-T to have limited efficacy in SCLC PDX models that did not express DLL3 and no cross-reactivity against DLL4. This suggests that tumor cell killing by Rova-T is mediated through DLL3 (23). Furthermore in our analysis, DLL3 expression was found to localize exclusively to the membrane and cytoplasm of the SC tumor component and was not expressed in the urothelial component, endothelium, or in adjacent normal tissue. We therefore hypothesize that DLL3-targeting agents would preferentially target the SC tumor component. If this is confirmed in future studies, therapy selection in SCBC may be driven by tumor SC%.

Published OnlineFirst October 16, 2018; DOI: 10.1158/1078-0432.CCR-18-1278



In the study described here, SCBC PDX models treated with a single dose of Rova-T showed durable repression of tumor growth relative to models treated with cisplatin/etoposide and models treated with humanized IgG control isotype (HuIgGLD6.5) with the same drug conjugate arm. This partial activity of HuIgGLD6.5, which has also been observed in other PDX models, could be explained by its ability to bind Fc-receptors expressed on myeloid cells. Presence of these myeloid cells in the PDX tumor environment could account for the observed nonspecific killing of tumor cells following release of the potent drug warhead in the tumor microenvironment (42). Furthermore, serial dilution experiments suggested that more durable repression of tumor growth with Rova-T relative to the control isotype may be due to more effective targeting of TIC by Rova-T. The data suggest the hypothesis that TICs may represent a potential DLL3-driven pathologic mechanism of tumor progression, which if adequately targeted with DLL3-specific agents may result in durable responses. Our preclinical data and the previously described efficacy of Rova-T in other small-cell and neuroendocrine malignancies support clinical trials in SCBC.

Our analyses had a number of limitations. As in all retrospective analyses, the full spectrum of confounding and selection biases is difficult to account for. The heterogeneity of the population that included localized and advanced disease, and diverse diagnostic, follow-up and treatment patterns, made meaningful comparisons of subpopulations impractical. The 23-year timespan of the cohort is challenging due to the dynamic diagnostic and treatment paradigms during this period. To some extent, this was offset by the fact that all tissues were independently reviewed and quantified by an experienced specialized pathologist using contemporary standards for SCBC diagnosis. Although costaining of biomarkers was not technically feasible, IHC of each biomarker was read by an experienced pathologist to reduce inter-observer variability. Microdissection of SC component was not performed prior to EdgeSeq analysis raising the question of SC tissue purity; however, gene expression patterns were analyzed along with SC%, and many of the clinical cases have mixed small-cell and urothelial histology. Finally, gene expression analysis was available in 39 of 63 patients raising the possibility of selection bias. However, the comparison of the 39-patient subset to the 63-patient overall cohort did not reveal substantial differences in clinicopathologic characteristics.

In summary, this was the first analysis to suggest that distinct gene expression patterns in SCBC identify more aggressive or indolent behavior and are associated with outcomes. We also report the frequency and prognostic value of DLL3, PDL1, CD56, and ASCL1 protein expression in SCBC. This work implicates increased DLL3 expression and increased CD56 expression as negative prognostic biomarkers. DLL3 may additionally be an important therapeutic target given its overexpression specifically on the SC component. We demonstrate the efficacy of a DLL3-targeting agent in a PDX model of SCBC. PDL1 assessment demonstrated lack of tumor cell staining consistent with literature in other neuroendocrine tumors showing relatively low IC expression with potential treatment implications (43). Our findings merit prospective validation and comprise an important step in understanding the biology of SCBC that may inform novel prognostic models, treatment paradigms, and clinical trial design.

## Disclosure of Potential Conflicts of Interest

L.R. Saunders has ownership interests (including patents) in AbbVie. A.J. Stephenson reports receiving speakers bureau honoraria from Genomic Health, and is a consultant/advisory board member for Astellas. A. Dowlati is a consultant/advisory board member for AbbVie and Takeda. P. Grivas reports receiving speakers bureau honoraria from Bristol-Myers Squibb and Genentech, is a consultant/advisory board member for AstraZeneca, Bayer, Biocept, Bristol-Myers Squibb, Clovis Oncology, Dendreon, Driver Inc., EMD Serono, Exelixis, Foundation Medicine, Genentech, Merck & Co., Pfizer, QED Therapeutics, and Seattle Genetics, reports receiving commercial research support from Clovis Oncology and Pfizer. No potential conflicts of interest were disclosed by the other authors.

## Authors' Contributions

**Conception and design:** V.S. Koshkin, J.A. Garcia, J. Reynolds, C. Magi-Galluzzi, J.K. McKenney, E. Bishop, L.R. Saunders, A.J. Stephenson, A. Dowlati, T. Gilligan, B.I. Rini, O.Y. Mian, P. Grivas

**Development of methodology:** V.S. Koshkin, J. Reynolds, J.K. McKenney, A.J. Stephenson, B.H. Lee, O.Y. Mian, P. Grivas

**Acquisition of data (provided animals, acquired and managed patients, provided facilities, etc.):** V.S. Koshkin, J.A. Garcia, J. Reynolds, C. Magi-Galluzzi, J.K. McKenney, K. Isse, E. Bishop, A. Balyimez, T. Gilligan, M.C. Ornstein, O.Y. Mian, P. Grivas

**Analysis and interpretation of data (e.g., statistical analysis, biostatistics, computational analysis):** V.S. Koshkin, J. Reynolds, P. Elson, C. Magi-Galluzzi, K. Isse, E. Bishop, L.R. Saunders, A. Balyimez, M. Hu, A.J. Stephenson, B.H. Lee, A. Dowlati, B.I. Rini, O.Y. Mian, P. Grivas

**Writing, review, and/or revision of the manuscript:** V.S. Koshkin, J.A. Garcia, J. Reynolds, P. Elson, C. Magi-Galluzzi, J.K. McKenney, K. Isse, L.R. Saunders, A. Balyimez, A.J. Stephenson, A.F. Fergany, B.H. Lee, G.-P. Haber, A. Dowlati, T. Gilligan, M.C. Ornstein, B.I. Rini, O.Y. Mian, P. Grivas

**Administrative, technical, or material support (i.e., reporting or organizing data, constructing databases):** V.S. Koshkin, P. Elson, S. Rashid, B.H. Lee, M.C. Ornstein, O.Y. Mian, P. Grivas, M.E. Abazeed

**Study supervision:** V.S. Koshkin, J.A. Garcia, C. Magi-Galluzzi, B.I. Rini, O.Y. Mian, P. Grivas, M.E. Abazeed

**Others (did some experiments in order to run the methylation sequencing):** S. Rashid

## Acknowledgments

The authors would like to thank Sam Williams, Marybeth Pysz, Hanna Ramoth, Tabita Popovici, Andrew Hsieh, and Lindsay Atkins for their contributions. This study was supported by the Bioinformatics, Imaging, and Integrated Genomics Shared Resources of the Case Comprehensive Cancer Center (P30 CA043703). This work was supported by a Velosano Foundation Cancer Research Award (to O.Y. Mian).

The costs of publication of this article were defrayed in part by the payment of page charges. This article must therefore be hereby marked *advertisement* in accordance with 18 U.S.C. Section 1734 solely to indicate this fact.

Received April 26, 2018; revised September 7, 2018; accepted October 8, 2018; published first October 26, 2018.

## References

1. Fahed E, Hansel DE, Raghavan D, Quinn DI, Dorff TB. Small cell bladder cancer: biology and management. Semin Oncol 2012;39:615–8.
2. Robertson AG, Kim J, Al-Ahmadie H, Bellmunt J, Guo G, Cherniack AD, et al. Comprehensive molecular characterization of muscle-invasive bladder cancer. Cell 2017;171:540–56.e25.
3. Meeks JJ, Lerner SP. Molecular landscape of non-muscle invasive bladder cancer. Cancer Cell 2017;32:550–1.
4. Cheng L, Pan CX, Yang XJ, Lopez-Beltran A, MacLennan GT, Lin H, et al. Small cell carcinoma of the urinary bladder: a clinicopathologic analysis of 64 patients. Cancer 2004;101:957–62.

5. Mukesh M, Cook N, Hollingdale AE, Ainsworth NL, Russell SG. Small cell carcinoma of the urinary bladder: a 15-year retrospective review of treatment and survival in the Anglian Cancer Network. BJU Int 2009; 103:747–52.
6. Abrahams NA, Moran C, Reyes AO, Siefker-Radtke A, Ayala AG. Small cell carcinoma of the bladder: a contemporary clinicopathological study of 51 cases. Histopathology 2005;46:57–63.
7. Lynch SP, Shen Y, Kamat A, Grossman HB, Shah JB, Millikan RE, et al. Neoadjuvant chemotherapy in small cell urothelial cancer improves pathologic downstaging and long-term outcomes: results from a retrospective study at the MD Anderson Cancer Center. Eur Urol 2013;64:307–13.
8. Siefker-Radtke AO, Dinney CP, Abrahams NA, Moran C, Shen Y, Pisters LL, et al. Evidence supporting preoperative chemotherapy for small cell carcinoma of the bladder: a retrospective review of the M. D. Anderson cancer experience. J Urol 2004;172:481–4.
9. Thota S, Kistangari G, Daw H, Spiro T. A clinical review of small-cell carcinoma of the urinary bladder. Clin Genitourin Cancer 2013;11:73–7.
10. Geynisman DM, Handorf E, Wong YN, Doyle J, Plimack ER, Horwitz EM, et al. Advanced small cell carcinoma of the bladder: clinical characteristics, treatment patterns and outcomes in 960 patients and comparison with urothelial carcinoma. Cancer Med 2016;5:192–9.
11. Bex A, Nieuwenhuijzen JA, Kerst M, Pos F, van Boven H, Meinhardt W, et al. Small cell carcinoma of bladder: a single-center prospective study of 25 cases treated in analogy to small cell lung cancer. Urology 2005;65:295–9.
12. Choong NWW, Quevedo JF, Kaur JS. Small cell carcinoma of the urinary bladder. The Mayo Clinic experience. Cancer 2005;103:1172–8.
13. Pasquier D, Barney B, Sundar S, Poortmans P, Villa S, Nasrallah H, et al. Small cell carcinoma of the urinary bladder: a retrospective, multicenter rare cancer network study of 107 patients. Int J Radiat Oncol Biol Phys 2015;92:904–10.
14. Mattes MD, Kan C-C, Dalbagni G, Zelefsky MJ, Kollmeier MA. External beam radiation therapy for small cell carcinoma of the urinary bladder. Pract Radiat Oncol 2015;5:e17–22.
15. Patel SG, Stimson CJ, Zaid HB, Resnick MJ, Cookson MS, Barocas DA, et al. Locoregional small cell carcinoma of the bladder: clinical characteristics and treatment patterns. J Urol 2014;191:329–34.
16. Siefker-Radtke AO, Kamat AM, Grossman HB, Williams DL, Qiao W, Thall PF, et al. Phase II clinical trial of neoadjuvant alternating doublet chemotherapy with ifosfamide/doxorubicin and etoposide/cisplatin in small-cell urothelial cancer. J Clin Oncol 2009;27:2592–7.
17. Meijer RP, Meinhardt W, van der Poel HG, van Rhijn BW, Kerst JM, Pos FJ, et al. Local control rate and prognosis after sequential chemoradiation for small cell carcinoma of the bladder. Int J Urol 2013;20:778–84.
18. Kollmeier MA. Counterpoint: is cystectomy needed for small-cell bladder cancer? Oncology 2015;29:648–9.
19. Raghavan D. Point: is cystectomy needed for small-cell bladder cancer? Oncology 2015;29:645–7.
20. Kouba EJ, Cheng L. Understanding the genetic landscape of small cell carcinoma of the urinary bladder and implications for diagnosis, prognosis, and treatment: a review. JAMA Oncol 2017;3:1570–8.
21. Teo M, Hao X, Desai N, Ostrovanaya I, Arora A, Funt S, et al. Small cell carcinoma of the bladder (SCCB): clinical, histopathologic, and genomic predictors of clinical outcomes. J Clin Oncol 2017;35:294–4.
22. Ladi E, Nichols JT, Ge W, Miyamoto A, Yao C, Yang LT, et al. The divergent DSL ligand Dll3 does not activate Notch signaling but cell autonomously attenuates signaling induced by other DSL ligands. J Cell Biol 2005; 170:983–92.
23. Saunders LR, Bankovich AJ, Anderson WC, Aujay MA, Bheddah S, Black K, et al. A DLL3-targeted antibody-drug conjugate eradicates high-grade pulmonary neuroendocrine tumor-initiating cells *in vivo*. Sci Transl Med 2015;7:302ra136.
24. Dylla SJ. Toppling high-grade pulmonary neuroendocrine tumors with a DLL3-targeted trojan horse. Mol Cell Oncol 2016;3:e1101515.
25. Rudin CM, Pietanza MC, Bauer TM, Ready N, Morgensztern D, Glisson BS, et al. Rovalpituzumab tesirine, a DLL3-targeted antibody-drug conjugate, in recurrent small-cell lung cancer: a first-in-human, first-in-class, open-label, phase 1 study. Lancet Oncol 2017; 18:42–51.
26. Pedersen N, Mortensen S, Sørensen SB, Pedersen MW, Rieneck K, Bovin LF, et al. Transcriptional gene expression profiling of small cell lung cancer cells. Cancer Res 2003;63:1943–53.
27. Peifer M, Fernández-Cuesta L, Sos ML, George J, Seidel D, Kasper LH, et al. Integrative genome analyses identify key somatic driver mutations of small-cell lung cancer. Nat Genet 2012;44:1104–10.
28. George J, Lim JS, Jang SJ, Cun Y, Ozretić L, Kong G, et al. Comprehensive genomic profiles of small cell lung cancer. Nature 2015;524:47–53.
29. Bourzac KM, Rounseville MP, Zarate X, Maddula VS, Henderson DC, Luckey JA, et al. A high-density quantitative nuclease protection microarray platform for high throughput analysis of gene expression. J Biotechnol 2011;154:68–75.
30. Roberts RA, Sabalos CM, LeBlanc ML, Martel RR, Frutiger YM, Unger JM, et al. Quantitative nuclease protection assay in paraffin-embedded tissue replicates prognostic microarray gene expression in diffuse large-B-cell lymphoma. Lab Invest 2007;87:979–97.
31. Pharmaceutical statistics: MBSW 39. Muncie, Indiana: Springer International Publishing; 2018.
32. U.S. Food and Drug Administration. VENTANA PD- L1 (SP263) Assay. Available from: https://www.accessdata.fda.gov/cdrh_docs/pdf16/p160046c.pdf.
33. U.S. Food and Drug Administration. VENTANA PD- L1 (SP142) Assay Available from: https://www.accessdata.fda.gov/cdrh_docs/pdf16/P160002c.pdf.
34. Kim KH, Roberts CWM. Targeting EZH2 in cancer. Nat Med 2016;22: 128–34.
35. Sato T, Kaneda A, Tsuji S, Isagawa T, Yamamoto S, Fujita T, et al. PRC2 overexpression and PRC2-target gene repression relating to poorer prognosis in small cell lung cancer. Sci Rep 2013;3:1911.
36. Coe BP, Thu KL, Aviel-Ronen S, Vucic EA, Gazdar AF, Lam S, et al. Genomic deregulation of the E2F/Rb pathway leads to activation of the oncogene EZH2 in small cell lung cancer. PloS One 2013;8:e71670.
37. Cancer Genome Atlas Research Network. Comprehensive molecular characterization of urothelial bladder carcinoma. Nature 2014; 507:315–22.
38. Chang MT, Penson A, Desai NB, Socci ND, Shen R, Seshan VE, et al. Small cell carcinomas of the bladder and lung are characterized by a convergent but distinct pathogenesis. Clin Cancer Res 2018;24:1965–73.
39. Faltas BM, Prandi D, Tagawa ST, Molina AM, Nanus DM, Sternberg C, et al. Clonal evolution of chemotherapy-resistant urothelial carcinoma. Nat Genet 2016;48:1490–9.
40. Saunders LR, Williams SA, Bheddah S, Isse K, Fong S, Pysz MA, et al. Expression of DLL3 in metastatic melanoma, glioblastoma and high-grade extrapulmonary neuroendocrine carcinomas as potential indications for rovalpituzumab tesirine (Rova-T; SC16LD6.5), a delta-like protein 3 (DLL3)-targeted antibody drug conjugate (ADC) [abstract]. In: Proceedings of the American Association for Cancer Research Annual Meeting 2017; 2017 Apr 1–5; Washington, DC. Philadelphia (PA): AACR; 2017. Abstract nr 3093.
41. Rovalpituzumab tesirine in delta-like protein 3-expressing advanced solid tumors - full text view - ClinicalTrials.gov. Available from: https://clinicaltrials.gov/ct2/show/NCT02709889?term=DLL3&rank=4.
42. Sharma SK, Chow A, Monette S, Vivier D, Pourat J, Edwards KJ, et al. Fc-mediated anomalous biodistribution of therapeutic antibodies in immunodeficient mouse models. Cancer Res 2018;78:1820–32.
43. Tsuruoka K, Horinouchi H, Goto Y, Kanda S, Fujiwara Y, Nokihara H, et al. PD-L1 expression in neuroendocrine tumors of the lung. Lung Cancer 2017;108:115–20.

AACR American Association for Cancer Research

Clinical Cancer Research

# Transcriptomic and Protein Analysis of Small-cell Bladder Cancer (SCBC) Identifies Prognostic Biomarkers and DLL3 as a Relevant Therapeutic Target

Vadim S. Koshkin, Jorge A. Garcia, Jordan Reynolds, et al.

*Clin Cancer Res* Published OnlineFirst October 16, 2018.